FINAL CONF-8509168--1

MEDIUM VOLTAGE ANALYTICAL ELECTRON MICROSCOPY MICROANALYSIS VERSUS RADIATION DAMAGE

Nestor J. Zaluzec, John F. Mansfield, Paul R. Okamoto, and Nghi Q. Lam
Materials Science and Technology Division
Argonne National Laboratory
Argonne, Illinois 60439 USA

CONF-8509168--1

DE85 018463

SEPTEMBER 1985

DISCLAIMER

*This work was supported by the U.S. Department of Energy, BES-Materials Sciences, under Contract W-31-109-Eng-38.

Submitted to EMAG 1985, University of Newcastle, Newcastle-upon-Tyne, England, Sept. 2-5, 1985.

Medium Voltage Analytical Electron Microscopy: Microanalysis versus Radiation Damage

N.J. Zaluzec, J.F. Mansfield, P.R. Okamoto and N.Q. Lam

Argonne National Laboratory, MST Division/212, Argonne, IL. 60439, USA

1. Introduction

During the last few years the manufacture of analytical microscopes operating at voltages (Vo) as high as 400 kV has progressed steadily. The motivation for this development is enhanced performance in image resolution and microanalysis relative to 100 kV operation. However, in the medium voltage regime the analyst must also be aware of the limitations imposed upon the experiments due to radiation damage effects. These effects can range from sputtering to radiation-induced segregation or electron beam-induced (compositional) mixing, localized to the vicinity of the probe. Since most analytical procedures used today assume that the incident beam does not alter the specimen composition, these deleterious effects can affect the validity of experimental results.

The benefits of higher voltage operation relative to x-ray and electron loss microanalysis have been discussed elsewhere (Zaluzec et al 1983, Zaluzec 1978) and include: increased characteristic signal due to relativisitic effects on the ionization cross-section and gun brightness, increased peak to background ratios due to anisotropic continuum emission, increased spatial resolution and decreased multiple scattering. The disadvantages are twofold. First, the generation of uncollimated radiation (Bentley et al 1979) will be more prolific and hence the precautions and modifications of the basic instrument become more complicated. Second, the effects of radiation damage (displacement versus ionization) become increasingly important as Vo increases. In displacement damage, kinetic energy is directly transfered from the incident electron to atoms within the solid. If the energy transfer is sufficient, then these atoms can be displaced from their lattice sites. At temperatures, where the defects are mobile, segregation to defect sinks can occur and structural or elemental rearrangement may result.

2. Results and Discussion

The kinetic energy transfered (T_I) to an atom by an electron of kinetic energy $T_E=eVo$ which has scattered through an angle ϕ is given by $T_I = [2*T_E*(T_E+2mo c^2)*\sin^2 \phi/2)]/[Mc^2]$ where M and mo are the masses of the target atom and electron. Table 1 documents the maximum energy which can be transfered to selected elements at various voltages for $\phi = 180^o$. These values should be compared with the critical displacement energy (T_d) required to permanently remove an atom from its site in a lattice and are also given therein. From the preceeding equation one can also calculate the minimum voltage (Vmin) required for T_I to exceed T_d, this value serves as a convenient reference point below which, one need not consider radiation damage. In addition, the values of T_d change with orientation and structure. Generally, the close-packed directions, <110> in FCC, and <100> in BCC have the lowest T_d values with other directions as much as 2-4 times higher.

The displacement rate of an atom is given by the product of its displacement cross-section (σ_d) multiplied by the electron current density. Values of σ_d (Oen, 1973) are generally in the range of 1 to 40 barns when $T_T > T_d$. The important point here, is that in probe forming systems, although σ_d is low, the probe current density can be sufficiently high to yield a significant displacement rate. For example, a current of 1 nA in a 20 nm diameter probe yields a current density of J=318 A/cm^2. Using these values, one calculates a displacement rate ($dx/dt = \sigma_d * J$), of 0.002 to 0.08 displacements/atom/sec (dpa/sec). In a 10^3 sec x-ray analysis, these dpa rates imply that <u>each atom</u> in the probe for which $T_T > T_d$ can be displaced from 2 to 80 times!

The important question, with respect to microanalysis, is how do these values compare with characteristic signal generation? For the case of X-ray analysis, figure 1 compares the calculated number of <u>detected</u> K-shell x-rays/e$^-$/atom from a 8 μm Be window SiLi detector subtending a solid angle (Ω) of 0.13 Sr (curve 1), with the maximum number of displacements/e$^-$/atom (curve 2) for Aluminium (fig. 1a) and Nickel (fig. 1b) as a function of voltage. The x-ray parameters (cross-section, etc) used in these calculations are documented elsewhere (Zaluzec, 1984). From this figure one can see that once Vo exceeds Vmin, the displacement rate quickly exceeds the x-ray detection rate. The relatively low x-ray signal is a consequence of the geometrical collection efficiency ($\varepsilon_\chi = \Omega/4\pi$ ~1%) of the SiLi detector as well as the x-ray fluorescence yield (ω_K). EELS, on the other hand, does not suffer these effects, having collection efficiencies ε_E ranging from 30-90% and a effective fluorescence yield of unity. The equivalent plot for EELS would lie above curve #1 by a factor of $\varepsilon_E/(\varepsilon_\chi * \omega_K)$ ~50X for Al and ~5X for Ni. In alloy systems, subthreshold displacement becomes another factor which must be considered when evaluating the importance of displacement damage. Here, atoms are displaced from their sites at voltages below Vmin. This effect occurs, in alloys, when lower-Z elements, which have undergone electron displacement, transfer their momentum by collisions with higher-Z species and subsequently cause the displacement of that element. This process will basically cause curve #2 to shift horizontally toward lower voltages and has not been included in these calculations since it is composition dependent.

The value for J given above is within the upper limit of some high intensity LaB_6 sources, however, for the case of Field Emission systems the current density can reach the range of 10^5 A/cm^2 and the corresponding displacement rates can then reach 50 - 100 dpa/sec! When a material is subjected to such severe conditions, it is highly unlikely that any phases within it remain stable. Observations have ranged from general mass loss experiments (Mochel et al 1983, Thomas 1985) to radiation-induced segregation (RIS) phenomena (Okamoto and Lam, 1985). The mechanism which dominates in a given situation depends on the irradiation conditions. At low defect recombination rates, particuliarly when the probe diameter is less than the specimen thickness, RIS becomes important as the defects have time to migrate away from the irradiation zone. At high displacement rate conditions, beam-induced mixing and/or sputtering will dominate. Unlike sputtering, the implications for AEM in the case of mixing and/or RIS are more subtle and also important for different reasons. First, we have a new high-resolution technique for changing the local composition. Second, we no longer have a nondestructive technique for microanalysis since the composition is changing during the measurement process!

An example of the RIS effect is given in figure 2 which shows a dark-field

time sequence depicting the microstructural evolution of an initially two phase Ni-12.7%Al alloy during HVEM irradiation at 700°C at 1 MV. The initially uniform two phase (γ ,γ' Ni_3Al) material segregates under the action of the incident electron probe forming a central Al-rich precipitate phase (γ') surrounded by a Ni-rich, γ' depleted zone. It has been shown (Okamoto and Lam, 1985) that this effect is due to radial displacement-rate gradients resulting form the Gaussian beam profile. For a focused electron beam, radial variations in the beam intensity (i.e. defect production rate) induce a radial outflux of point defects from the irradiated area. In Ni binary alloys, this defect flux results in a radial influx of oversized solutes like Al into the regions of the irradiated zone where the beam intensity profile (or the defect concentration, C_d) is concave downward. The resulting solute concertration in the Ni-Al alloy is proportional to the divergence of the defect gradient $\nabla^2 C_d$; oversize solute enrichment occurs in regions where $\nabla^2 C_d < 0$ and depletion in regions where $\nabla^2 C_d > 0$. The kinetics of this effect is particuliarly strong, increasing as the probe diameter decreases and/or the current density increases, at temperatures where defects are mobile. Similiar results have also been obtained at 300 kV in an Al-1.95%Zn alloy at ~160°C as shown in figure 3. Here a variation in the measured characteristic x-ray intensity ratio of Zn/Al with time indicates a change in composition due to RIS and provides the first experimental evidence that in modern AEM type instruments, appropriate caution must be exercised.

Additional research on these topics is continuing. This work was supported by the U.S. Department of Energy at Argonne National Laboratory.

3. References

Bentley J., Zaluzec N., Kenik E., Carpenter R.,SEM/1979/I, pge 581, 1979
Mochel M.E., Humphreys C.J., Eades J.A., Mochel J.M., Petford A.M., App. Phys. Let., Vol 42 (4) pge 392 (1983)
Oen O.S., OakRidge Nat. Lab. Report,#TM-4897, 1973
Okamoto P., Lam N., Proc. Mat. Res. Soc. Sym. Vol. 41 pge 241, 1985
Thomas L.E., Proc. of ASU HREM Symp., (in press Ultramicroscopy) 1985
Zaluzec N.J., Taylor A., Ryan E., Phillipides A., Proc. 7th HVEM meeting, Univ. of Calif.,Berkeley CA. #LBL-16031 CONF-830819 pge 79, 1983
Zaluzec N.J. 9th Int. Cong. on EM, Toronto Canada, pge 548, 1978
Zaluzec N.J. EMSA Bulletin Vol. 14, No. 1,pge 67,Vol. 14 No. 2 pge 61,1984
Zaluzec N.J. Proc. of AEM Workshop July 1984, Lehigh University, Bethelehem Pa, San Francisco Press, pge 279, 1984

Table 1
Maximum Kinetic Energy Transferable to Selected Elements

Atom	M	100 kV	200 kV	300 kV	400 kV	Td	Vmin
C†	12.01	20.1[eV]	43.7	71.0	101.8	30	145
O	15.99	15.1	32.8	53.2	76.4	--	---
Al	26.98	8.9	19.5	31.6	45.3	16	180
Ti	47.90	5.0	11.0	17.8	25.5	15	270
Ni	58.71	4.1	8.9	14.5	20.8	24	450
Mo	95.94	2.5	5.5	8.9	12.7	37	875
Ag	107.8	2.2	4.9	7.9	11.3	28	770
Au	196.9	1.2	2.7	4.3	6.2	34	1300

† = Graphite

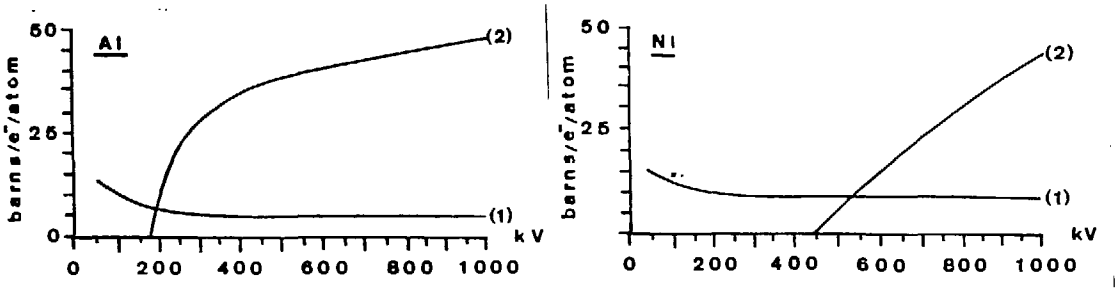

Figure 1. Calculation of the number of detected Kα x-rays/e⁻/atom (#1) and number of displacements/e⁻/atom (#2) for Aluminium and Nickel versus Vo.

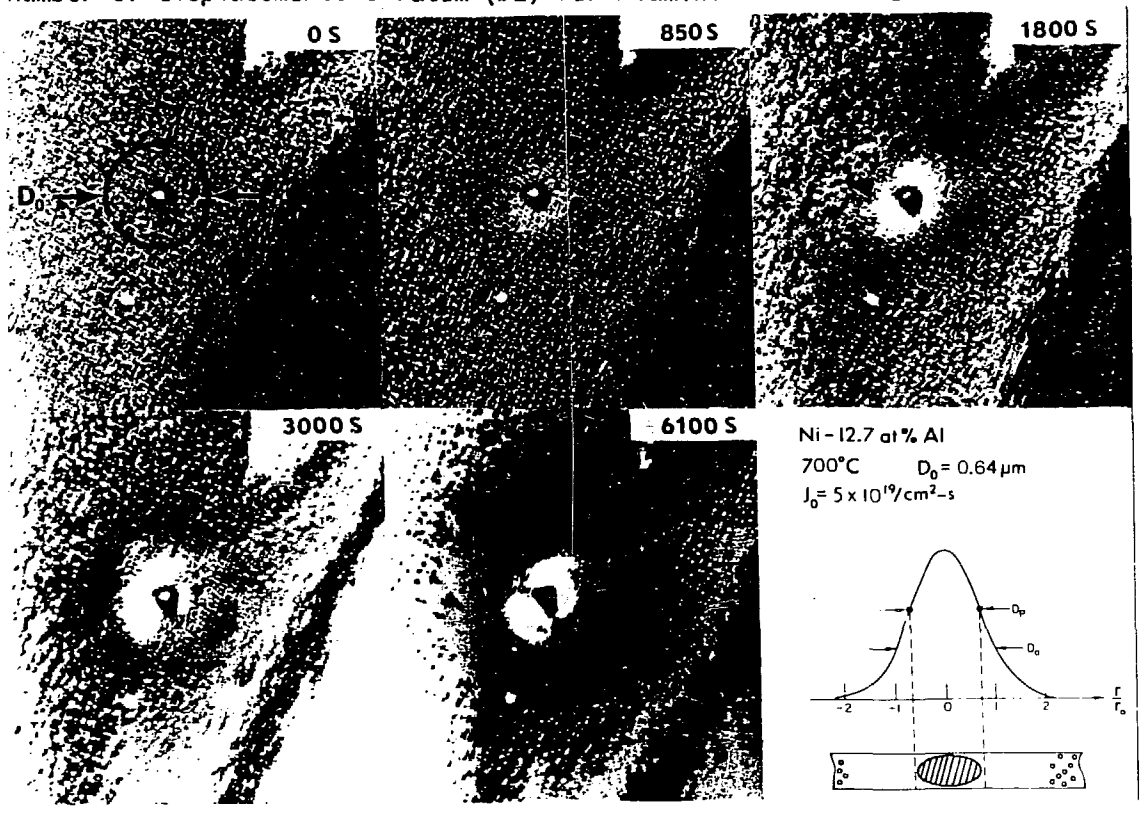

Figure 2.Dark-field (γ'reflection) micrographs showing the development of RIS due to displacement rate gradients in Ni-12.7%Al during 1 MV HVEM irradiation at 700°C. The incident beam diameter is shown by the circle marked Do.

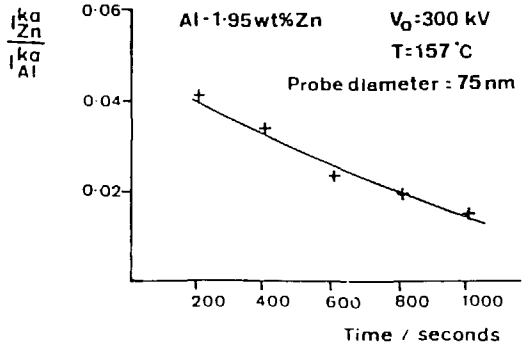

Figure 3. Measured variation of the Zn/Al Kα intensity ratio as a function of time (200 sec intervals) during 300 kV irradiations of Al-1.95%Zn at ~160°C in a medium voltage TEM with a 75 nm diameter probe.